Eur Biophys J (2012) 41:959–968
DOI 10.1007/s00249-012-0854-0

ORIGINAL PAPER

EBSA
Biophysics in Europe

κ-Casein terminates casein micelle build-up by its "soft" secondary structure

Krisztina Nagy · György Váró · Balázs Szalontai

Received: 15 February 2012 / Revised: 11 June 2012 / Accepted: 11 June 2012 / Published online: 27 September 2012

Abstract In our previous paper (Nagy et al. in J Biol Chem 285:38811–38817, 2010) by using a multilayered model system, we showed that, from α-casein, aggregates (similar to natural casein micelles) can be built up step by step if Ca-phosphate nanocluster incorporation is ensured between the protein adsorption steps. It remained, however, an open question whether the growth of the aggregates can be terminated, similarly to in nature with casein micelles. Here, we show that, in the presence of Ca-phosphate nanoclusters, upon adsorbing onto earlier α-casein surfaces, the secondary structure of α-casein remains practically unaffected, but κ-casein exhibits considerable changes in its secondary structure as manifested by a shift toward having more β-structures. In the absence of Ca-phosphate, only κ-casein can still adsorb onto the underlying casein surface; this κ-casein also expresses considerable shift toward β-structures. In addition, this κ-casein cover terminates casein aggregation; no further adsorption of either α- or κ-casein can be achieved. These results, while obtained on a model system, may show that the Ca-insensitive κ-casein can, indeed, be the outer layer of the casein micelles, not only because of its "hairy" extrusion into the water phase, but because of its "softer" secondary structure, which can "occlude" the interacting motifs serving casein aggregation. We think that the revealed nature of the molecular interactions, and the growth mechanism found here, might be useful to understand the aggregation process of casein micelles also in vivo.

K. Nagy · G. Váró · B. Szalontai (✉)
Institute of Biophysics, Biological Research Centre,
Hungarian Academy of Sciences, P.O.B. 521,
Szeged 6701, Hungary
e-mail: szalontai.balazs@brc.mta.hu

Keywords α-Casein · κ-Casein · Casein micelle · Atomic force microscopy (AFM) · Attenuated total reflection Fourier-transform infrared (ATR-FTIR)

Introduction

Caseins, the most abundant proteins in milk, are responsible for the transport of calcium phosphate (CaP), which is essential for bone development of mammalian neonates. In milk, caseins form micelles, which have roughly spherical shapes and whose sizes may vary between 150 and 300 nm. These casein micelles can be made up from four different caseins [α(s1), α(s2), β, and κ] (Walstra and Jennes 1984). α-Casein and β-casein are calcium sensitive, while κ-casein is insensitive to calcium. As the principle of casein micelle organization, two alternative models have emerged (for reviews see Farrell et al. 2006; Horne 2002, 2006; Walstra 1999). According to the submicelle model, caseins first form small subunits called submicelles (∼15–20 nm); these units are then connected with each other, forming the micelles (Walstra 1999). Recently, the coexistence of submicelles with casein micelles in thin, spin-coated films has been shown (Müller-Buschbaum et al. 2007). The other—copolymer—model does not assume submicelles; it rather considers the CaP nanoclusters as nuclei for micelle growth by making contact with the phosphoseryl residues of several casein molecules (Holt et al. 2003).

Previously, we found ∼20-nm-sized features in α-casein films, which were built layer by layer from very dilute (0.1 mg ml^{-1}) solution onto polyelectrolyte films (Nagy et al. 2010). In all those experiments, first, CaP nanoclusters had to be formed on the surface of the terminating layer, and then α-casein could adsorb again. If the

negative phosphoseryl residues—required for CaP binding—were blocked (e.g., by adsorbing α-casein onto a positively charged polyelectrolyte film, where the casein–film interaction involved these residues), there was no way for any further building of α-casein multilayers (with or without the presence of CaP nanoclusters).

On the basis of these findings, we proposed a mechanism for the casein micelle build-up: the process starts by forming small aggregates (up to ~20 nm), in which the hydrophobic parts of the amphipathic α-caseins take part (this view resembles that proposed by Waugh 1970). These aggregates have their phosphoseryl residues on their hydrophilic surfaces. The phosphoseryl residues bind the CaP nanoclusters, which will also create a negative surface. The next adsorbing layer of α-caseins will bind to these negative surfaces by their positive groups, leaving their phosphoseryl residues free for other CaP binding, and so on. This scheme emerged from results obtained by Fourier-transform infrared spectroscopy monitoring of sequential adsorption of α-casein layers. With step-by-step adsorption events, we tried to imitate the real aggregation process leading to casein micelles. This model represented something "in between" the existing submicelle and copolymer models for casein micelle formation (Nagy et al. 2010).

However, we could not show (and this is a problem of the other micelle models as well) how the growth of our construction, which seemingly could go on as long as the components were available, could be terminated, i.e., how a Ca-insensitive surface, a prerequisite for having stable casein micelles in milk, could be obtained.

Former studies have shown that the outer layer of the casein micelles is made up of κ-casein (Holt and Horne 1996; Walstra 1990), which is very important from the point of view of the stability of the micelles (De Kruif and Zhulina 1996). The structural model of κ-casein (Farrell et al. 2012) revealed that it is made of two domains: one is hydrophobic but nevertheless carries a net positive charge, and interacts strongly with other casein molecules (residues 1–95); the other carries a net negative charge and contains mostly polar residues (113–169). These two domains are connected by a third one (96–112) containing a target motif for chymosin (Farrell et al. 2012). In κ-casein, the amount of the extended or β-sheet is relatively high (~30 %) (Farrell et al. 2003), including the connecting domain, where—according to molecular model calculations (Palmer et al. 2010)—extended structure is needed for chymosin cleavage (the basic reaction for milk clotting). Thus, looking for altered features appearing upon κ- ↔ α-casein interaction (as compared with that of α- ↔ α-casein), and for changes in the secondary structure of the (α–κ)-casein complexes, might provide a clue to reveal the specific structural role of κ-casein in casein micelle formation.

Toward this end, we built multilayers from α- and κ-caseins in the presence/absence of CaP nanoclusters between the adsorption steps. It turned out that, upon α- ↔ κ-casein interaction, the secondary structure of the κ-casein is more volatile for shifting toward β-sheets. We could show that, in the presence of CaP, both α- and κ-casein can be incorporated unlimitedly into multilayered architectures. However, in the absence of CaP, only κ-casein—in a small amount—could bind onto the α-casein surface, while in the opposite order there was no adsorption at all. In addition, it could be shown that only κ-casein adsorption induces a structural change in the architecture, namely a shift toward more β-sheets. Our findings support former studies (e.g., Holt and Horne 1996) with direct experimental evidence that κ-casein, indeed, can be the terminating component, thus providing a Ca-insensitive surface for casein micelles.

Experimental procedures

Polyelectrolyte films

For the experiments, PEI-$(PSS/PAH)_6$ or PEI-$(PSS/PAH)_5$-PSS films were constructed from 1 mg ml^{-1} solutions of the polyelectrolytes [PEI = poly-(ethyleneimine), MW = 750,000 g mol^{-1}; PSS = poly-(sodium-4-styrenesulfonate), MW = 70,000 g mol^{-1}; PAH = poly-(allylaminehydrochloride), MW = 60,000 g mol^{-1}].

For Fourier-transform infrared (FTIR) measurements, polyelectrolyte films were built up with the layer-by-layer method (Decher 1997) by adsorbing the polyelectrolytes onto the surface of the ATR crystal from solutions circulated by a peristaltic pump as earlier (Schwinte et al. 2001). After the deposition of each polyelectrolyte layer, a single-beam infrared spectrum was recorded to monitor the build-up of the film. Each adsorption step was separated by an extensive washing period using 10 mM H_2O-based 4-(2-hydroxyethyl)-1-piperazineethanesulfonic acid (HEPES) buffer (pH 7.0). After its construction was completed, the film was washed with D_2O-based HEPES buffer, and a single-beam infrared spectrum was recorded as reference for the later protein spectra.

For atomic force microscopy (AFM), freshly cleaved 1 × 1 cm^2 mica (SPI-Chem™ mica sheets; Structure Probe, Inc., West Chester, PA, USA) surfaces were used as supports for the polyelectrolyte films. Details of polyelectrolyte film preparation are given in Nagy et al. (2010). Briefly, the polyelectrolyte film was started by adsorbing PAH onto the mica from 400 µl volume, then the surface was washed twice with HEPES buffer (10 mM, pH 7). After washing, PSS was adsorbed onto the PAH layer also from 400 µl volume, again followed by washing. These

steps were repeated until the $(PAH/PSS)_6$ architecture was achieved. Finally, α- or κ-casein was adsorbed from 400 µl solution of 0.1 mg ml^{-1} concentration. Washing with the same buffer separated each protein adsorption step.

Casein solutions

Bovine milk α-casein (Sigma, C6780, α_s-casein minimum 70 %), and κ-casein (Sigma, C0406, minimum 80 % κ-casein) were purchased in lyophilized form, and their purity was checked by sodium dodecyl sulfate (SDS) gel electrophoresis (data not shown) and found sufficient, thus they were used without any further purification. In native polyacrylamide gel (1 % cross-linking, conc. 7 %) κ-casein showed polymers, most of them running together with bovine serum albumin (BSA) dimers. Caseins were always dissolved in D_2O-based HEPES buffer (10 mM) at pD 7.0. The concentration of the casein solutions was 0.1 mg ml^{-1} in all experiments. All other chemicals were also from Sigma-Aldrich (Germany).

Calcium phosphate (CaP) nanocluster formation

CaP nanoclusters were formed as described earlier on protein surfaces by circulating high concentration of Ca^{2+} ions in the form of 1 M $CaCl_2$. Then, without washing away the Ca solution, a solution of 50 mM Na_2HPO_4 was introduced into the sample holder by a peristaltic pump. All white precipitate (i.e., the excess insoluble fraction of the formed CaP) was removed by washing the film thoroughly with HEPES buffer. The characteristic phosphate vibrational bands in the 1,200–1,000 cm^{-1} region of the infrared spectrum, recorded after the washing, evidenced the presence of CaP on the protein surface (for details see Nagy et al. 2010).

Attenuated total reflection Fourier-transform infrared (ATR-FTIR) spectroscopy

On a Bruker Vertex 70 Fourier-transform infrared spectrometer, for each measurement 2,048 interferograms at 2 cm^{-1} spectral resolution were collected, summed up, and transformed into single-beam intensity spectra. As internal reflection element, a trapezoid ZnSe crystal (45°, six reflections) was used. Due to the long duration of the experiments, inevitably water vapor bands appeared in the spectra (in the range of mOD), in spite of the continuous purging of the spectrometer with dry air. These water vapor bands were removed in two steps: first, by interactive vapor spectrum subtraction via the Bruker Opus software, then by stationary wavelet transform denoising as described earlier in detail (Nagy et al. 2010). To ensure comparability, especially of the second derivatives, all infrared spectra shown in the present study were denoised at level 5, based on the eighth member of the Daubechies wavelet family (Mallat 1998). Other spectrum processing (baseline subtraction, taking second derivatives, etc.) was carried out with SPSERV software (Dr. Cs. Bagyinka, BRC Szeged, Hungary). All FTIR experiments were carried out at room temperature. All casein spectra were recorded in D_2O environment, therefore amide I bands are indicated as amide I′ throughout the paper. The difference absorption spectra of a given layer shown in the figures were calculated by taking always the last single-beam spectrum recorded before the adsorption of the layer as background, and the single-beam spectrum recorded after the adsorption as sample.

Singular value decomposition (SVD) analysis

The changes induced in the infrared spectra by the adsorption steps were evaluated by SVD analysis (Henry and Hofrichter 1992). The calculations were carried out with the SPSERV software. Briefly, if a system as a function of an external parameter (in the present case: the layer number of the protein multilayer) contains s_i species, which are spectrally distinguishable at any layer, the measured spectrum can be described as a linear combination of these s_i species. The output of the SVD analysis is a reduced representation of the data matrix in terms of a set of s_i basis spectra, an associated set of layer-dependent amplitude vectors (v_i), and a diagonal matrix with the weights (w_i). Since the set of output components is ordered by decreasing size, each subset consisting of the first j components provides the best j-component approximation of the data matrix. For a deeper understanding of the SVD method, see our earlier works where we applied SVD analysis to the gel-to-liquid crystalline phase transition of dipalmitoylphosphatidylcholine (Kota et al. 1999), or to protein denaturing and lipid–protein interactions in biological membranes (Szalontai 2009).

In our case, when the spectral changes appearing upon the build-up of the protein multilayer are to be analyzed, the s_1 basis spectrum shows an average of all layers; s_2 shows the largest changes upon the build-up, which have to be linearly combined with the s_1 spectrum to get the actual spectrum at a given layer. The v_2 amplitude vector gives the layer dependence of the largest change, manifested in the s_2 spectrum, etc. In the present case, we restricted ourselves to the s_1, s_2 spectra; even the corresponding v_1 and v_2 vectors were not considered due to the small number of layers.

Atomic force microscopy (AFM)

Atomic force microscopy measurements were carried out on an Asylum MFP-3D head and controller (Asylum

Research, Santa Barbara, CA). The driver program MFP-3D Xop was written in IGOR Pro software (version 6.22a; Wavemetrics, Lake Oswego, OR, USA). Gold-coated, silicon nitride rectangular cantilevers were used with a typical spring constant of 30 pN nm^{-1}, and with tip radius ~30 nm (BL-RC150 VB–C1: Bio-Lever A; Olympus Optical Co. Ltd., Tokyo, Japan). The spring constant for each cantilever was determined by thermal calibration (Butt and Jaschke 1995; Florin et al. 1995; Hutter and Bechhoefer 1993). The measurements were carried out in tapping mode under liquid at room temperature. Typically, 512 × 512 point scans were taken at a scan rate of 1 Hz per line. Both trace and retrace images were recorded and compared. To characterize the changes in the mechanical properties of the protein multilayers, the elastic (Young's) modulus was determined by force measurements as described in details previously (Nagy et al. 2010).

Results

Casein adsorption onto positively charged polyelectrolyte surface (PAH-ending film)

Earlier, we found that adsorption onto a positive surface blocks α-casein's ability to establish contacts with CaP nanoclusters or other α-casein molecules (Nagy et al. 2010). Here, we first checked whether this is true for the interaction with κ-casein as well.

In Fig. 1, it can be seen that, while a considerable amount of α-casein adsorbs onto the PAH-ending, positive polyelectrolyte surface, there is no CaP nanocluster adsorption onto this casein (see the lack of phosphate-related bands in the 1,200–1,000 cm^{-1} region). There was no adsorption either from α- or κ-casein solutions circulating above the first α-casein layer. It seems that, in line with our earlier findings (Nagy et al. 2010), α-casein when bound to a positive surface, indeed loses its capacity for interacting with other proteins needed for micelle formation.

Therefore, all the following ATR-FTIR experiments were carried out on PSS-ending PEI-$(PAH/PSS)_6$ polyelectrolyte film architecture having a negatively charged surface.

Aggregation of α- and κ-caseins in the presence of CaP nanoclusters (PSS-ending films)

First, as a control, consecutive layers of α-casein were adsorbed onto the PSS-ending, negatively charged polyelectrolyte surface (upper panel of Fig. 2a). As can be seen, large and increasing amounts of α-casein were adsorbed if CaP nanoclusters were formed on the surface of each

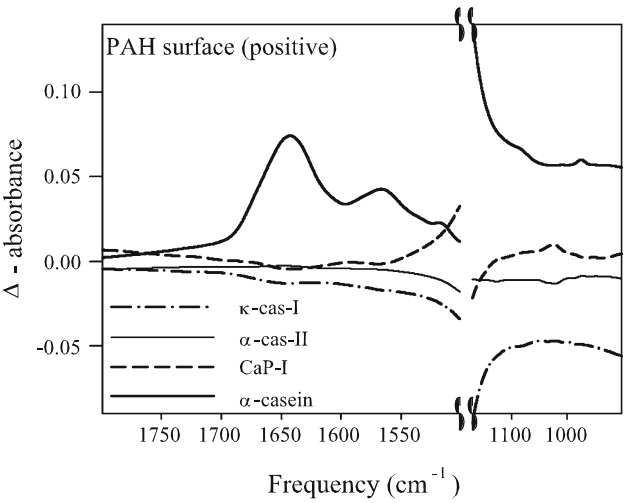

Fig. 1 Absorption changes in the amide I′ and the phosphate vibrational regions of the ATR-FTIR spectra of α– and κ-casein adsorbed onto PAH-ending (positively charged) polyelectrolyte film surface. Here, and in all other figures, the starting protein of a multilayer architecture is indicated by the full name (here *α-casein*); the consecutive layers, from the *bottom upward*, are given only with abbreviations (*CaP-i*; *x-cas-j*). In all experiments, absorption steps were separated by thorough washing with 10 mM HEPES buffer at pD 7.0. Note, that after the first adsorption step, the characteristic amide I′ band at around 1,650 cm^{-1} appears (*α-casein*). In contrast, the infrared spectra recorded upon following adsorption attempts could not exhibit any additional adsorbed material: neither CaP in the 1,200–1,000 cm^{-1} phosphate region (*CaP-I*) nor α-casein or κ-casein [see the flat in the amide I′ regions of (*α-cas-II*) and (*κ-cas-I*), respectively]. [For the otherwise appearing intense phosphate-related IR bands see our previous work (Nagy et al. 2010)]

adsorbed α-casein layer before the next adsorption step (see α-casein and α-cas-II spectra in Fig. 2a).

If the consecutive protein layers were intercalated by a CaP nanocluster-forming step, the amounts of adsorbed α- and κ-caseins were similar, and the construction of the protein multilayer could go on, apparently unlimitedly. There was, however, a very important difference between α- and κ-casein. When κ-casein was adsorbed, the frequency of its amide I′ band maximum considerably downshifted in the consecutive layers of the build-up. The reference spectrum of κ-casein, adsorbed alone onto an identical polyelectrolyte film in a separate experiment, is given in the lower panel of Fig. 2a.

An inherent feature of this type of infrared measurements is that the difference seen between two adsorption steps is the total change appearing upon the given adsorption. In general, it is impossible to localize where the changes took place, i.e., only in the newly adsorbed layer, in the underlying, earlier layers, or in both. Nevertheless, here we can assign the observed downshift to changes in the κ-casein structure, since when α-casein is put on the top of κ-casein, there is no further downshift; instead, the

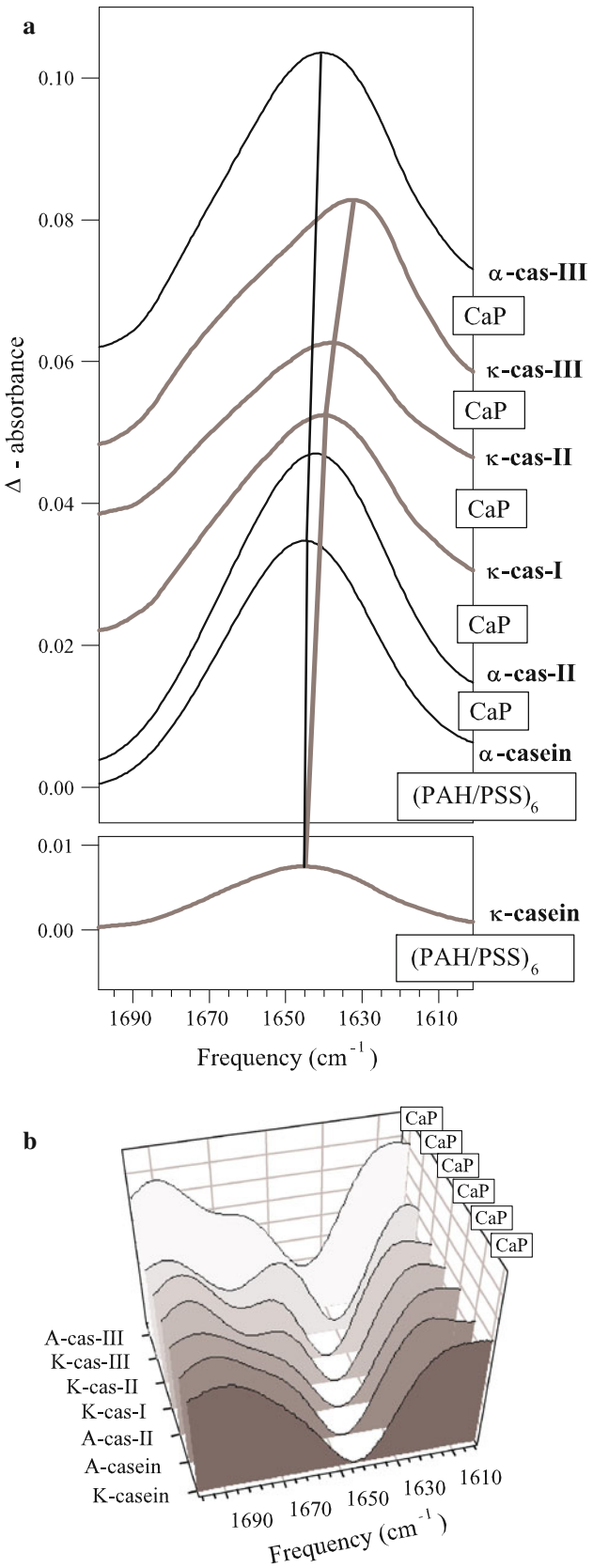

◀ **Fig. 2** Structural changes in α- and κ-casein upon the build-up of their multilayers in the presence of CaP nanoclusters. **a** Amide I′ absorption increments upon α- or κ-casein adsorption steps separated by CaP nanocluster formation. For comparison, the *lower panel* shows the amide I′ region of κ–casein from a separate experiment on the surface of an identical polyelectrolyte film. Polyelectrolyte film architectures, the sequence of casein adsorption steps, and of CaP nanocluster formation (CaP) are indicated along the right *y* axis starting from the bottom. For clarity, the spectra are vertically displaced. **b** Second derivatives of the infrared spectra depicted above. Note that, besides the downshift of the major minimum, upon the build-up of the multilayer, a second minimum emerges at around 1,670 cm^{-1} in κ-casein. This pair of low- and high-frequency components is indicative of *β*-sheet formation. Note also that the final *α-cas-III* more or less preserves the original α-casein structure, and the major minimum returns toward higher frequencies seen for α-casein

frequency of the amide I′ band of the last adsorbed α-casein is again very close to that of the first α-casein layer.

Inspection of the second derivatives of the amide I′ bands (Fig. 2b) reveals that the secondary structures of κ- and α-casein are very similar when they are alone on the polyelectrolyte film and there is no CaP present (κ-casein and α-casein curves in Fig. 2b, from two different experiments). It has to be mentioned here that Fig. 2b presents a low resolution of the amide I′ band, since the spectra were wavelet denoised (see "Experimental procedures"), and there was a nine-point smoothing when taking the second derivative. However, taking into account their intrinsically disordered nature (Tompa and Fuxreiter 2008), we thought that demonstrating only the major changes is sufficient for caseins. When building a protein multilayer architecture (starting from α-casein in Fig. 2b), the second derivatives of the first two α-casein layer spectra are very similar. A major change appears when κ-casein is adsorbed onto α-casein (κ-cas-I-II-III in Fig. 2b). Besides the downshift of the major minimum to about 1,630 cm^{-1}, a new minimum appears around 1,670 cm^{-1}. This pair of bands is characteristic of antiparallel *β*-structures (Arrondo et al. 1993). α-Casein adsorption onto κ-casein reversed the tendency of containing more and more *β*-sheets in the protein multilayer; instead of further downshift, the major minimum of the second derivative of the last α-casein layer (α-cas-III in Fig. 2b) is at similarly high frequency to that of the first α-casein layer.

A more detailed analysis and separation of the α- or κ-casein-related structural changes upon the build-up of the protein multilayer could be achieved by decomposing the recorded infrared spectra to singular values (SVD analysis). To set the starting situation, the normalized infrared absorption spectra of the amide I′ regions of α- and κ-casein are shown in Fig. 3a. These spectra were recorded when the α- or κ-casein was adsorbed alone onto the

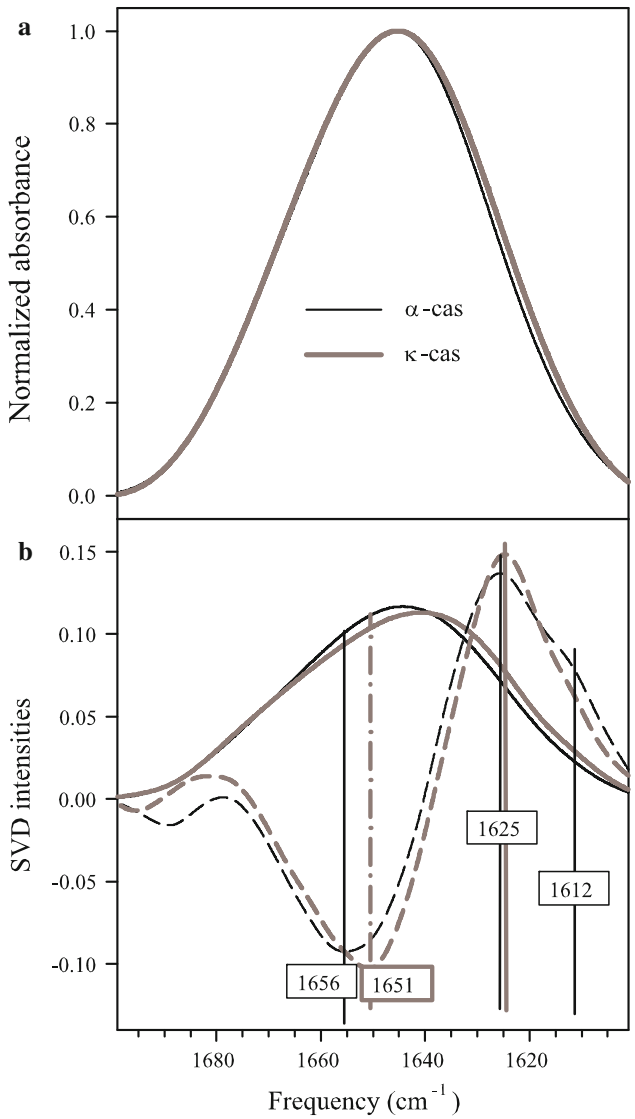

Fig. 3 SVD analysis of the amide I′ regions of the infrared spectra of α- and κ-casein shown in the upper panel of Fig. 2a. **a** Normalized infrared absorption spectra of the amide I′ regions of α- and κ-casein, each adsorbed alone onto a $(PAH/PSS)_6$ polyelectrolyte surface (note how similar they are). **b** For α-casein: (*black straight line*) the average shape (s_1 basis spectrum, *black broken line*) the largest change (s_2 basis spectrum) over *α-cas-I-II-III* layers shown in Fig. 2a; For κ-casein: (*gray straight line*) the average shape (s_1 basis spectrum, *gray broken line*) the largest change (s_2 basis spectrum) over κ-casein and *κ-cas-I-II-III* layers shown in Fig. 2. Note that these spectra, reflecting interaction-induced changes, are considerably different for α- and κ-casein

surface of a $(PAH/PSS)_6$ polyelectrolyte film. As can be seen, the amide I′ regions of the two caseins are very similar to each other: only the low-frequency side of the amide I′ band exhibits slightly higher absorption in κ-casein.

For the SVD analysis, the spectra shown in Fig. 2a were separated into two sets, containing only either α- (α-casein and α-cas-II-III) or κ-casein (κ-casein and κ-cas-I-II-III) spectra. The results of the SVD analysis of these two sets are shown in Fig. 3b. The curves with continuous lines show the first basis spectra (the "average") obtained from the SVD analysis. It can be seen that the average of the κ-casein spectra (gray line) is shifted toward lower frequencies as compared with the α-casein average (black line). This means that the structure of κ-casein deviates more from its original upon the consecutive adsorption steps of the build-up of the casein multilayer. More interesting are the curves (dashed lines) that show the second basis spectra (the largest variation) obtained from the SVD analysis: According to these curves (Fig. 3b), the largest spectral change upon building up the protein multilayer is the emergence of β-structures at the cost of loss of intensity at around 1,656 or 1,651 cm^{-1} in α- and κ-casein, respectively. [This tentative β-sheet assignment is based on the similarity of the frequencies of the emerging features at around 1,625 and 1,680 cm^{-1} in the s_2 spectra to those frequencies assigned to β-sheets in the protein infrared spectra (Arrondo et al. 1993).] The difference between their second basis spectra clearly shows that the domains, which suffer changes upon aggregation needed for the protein multilayer, are different in the two caseins. (This might seem to be a not very specific statement, but we think that, instead of moving into the shaky terrain of determining percentages of poorly identifiable secondary structure elements, the SVD method, which deals with these changes and does not require any precondition or arbitrary data manipulation, may provide maybe less secondary structure-specific but more solid information concerning the differences between α- and κ-casein.)

Due to the algorithm of the SVD decomposition, the obtained basis spectra are in a way normalized, thus from Fig. 3b it is not evident that the changes were much larger in κ-casein than in α-casein. The magnitude of the change can be seen from the proportion of the weights of the second and the first basis spectra (w_2/w_1), which was $0.73/14.8 = 0.05$ for α-casein and $1.42/17.3 = 0.08$ for κ-casein.

κ-Casein adsorption onto α-casein without CaP nanoclusters

To terminate micelle build-up, κ-casein should be able to adsorb onto α-casein even without the presence of CaP nanoclusters. An experiment showing that indeed this is the case is depicted in Fig. 4. First, as a control, two α-casein layers were put onto the polyelectrolyte film in the presence of CaP nanoclusters (α-casein and α-cas-II curves in Fig. 4a). Then, after thorough washing, an attempt was made to adsorb α-casein again, with no result (α-cas-III). κ-Casein, however, albeit in much lower amount than in the

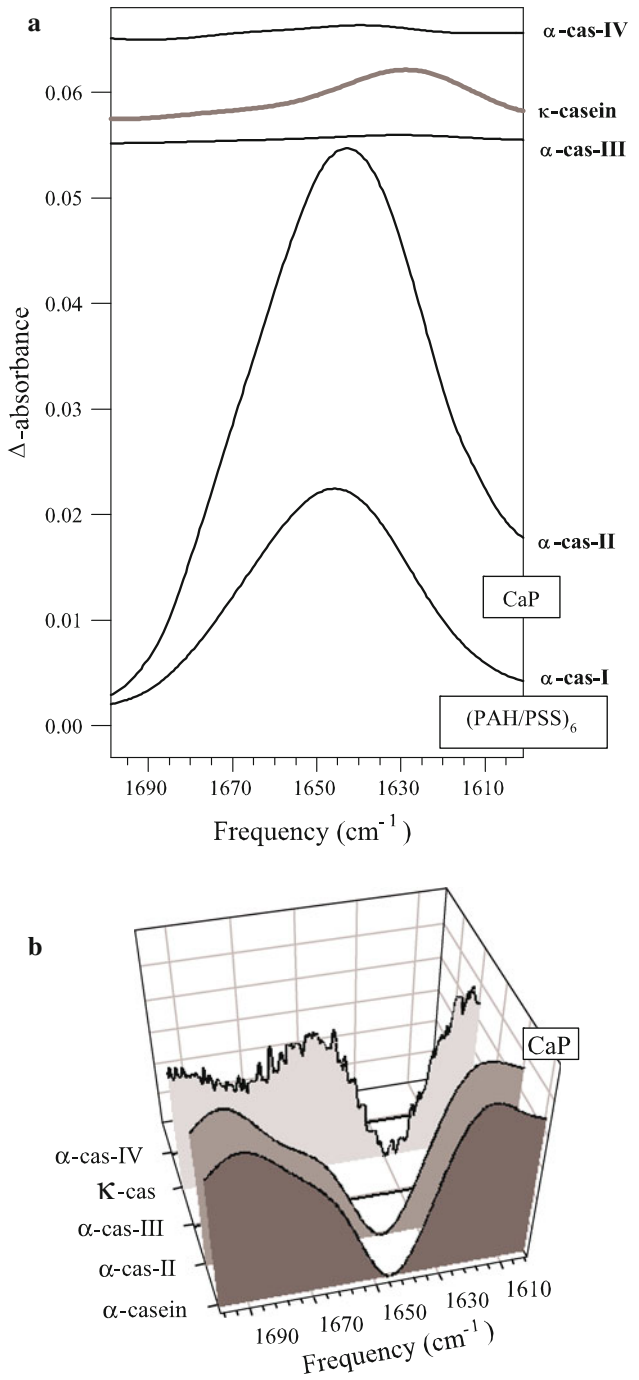

Fig. 4 κ-Casein adsorption onto α-casein in the absence of CaP nanoclusters. **a** Amide I′ region of the incremental infrared spectra upon the construction of the protein multilayer. Steps of the architecture build-up are indicated along the right *y* axis as in Fig. 2. Washing with 10 mM HEPES pH 7.0 followed each adsorption event, and infrared spectra were recorded in the presence of this buffer. Note that, without CaP nanocluster formation, there was very little α-casein adsorption (*α-cas-III*); only κ-casein could be adsorbed (*κ-casein*) in considerable amount. **b** Second derivatives of the amide I′ regions. For clarity, the derivatives of *α-cas-III* and *α-cas-IV*, due to their very low adsorption increments, are omitted. The higher noise of *κ-cas* is due to the lower signal-to-noise ratio of the original infrared absorption spectrum

presence of CaP, did adsorb onto the CaP-free α-casein surface (κ-cas curve in Fig. 4a). The downshift of the κ-casein amide I′ band toward β-structures was similar here to that found in the presence of CaP. Onto this κ-casein, only a minute amount of α-casein could adsorb (α-cas-IV in Fig. 4a). Therefore, one may conclude that κ-casein terminated the construction of the protein multilayer.

As regards the secondary structures of the different elements of the architecture, the similarity of the α-caseins (α-casein and α-cas-II) in Fig. 4b to those shown in Fig. 2 is expected, since there were CaP nanoclusters between them in both cases. When κ-casein was adsorbed without the "aid" of CaP nanoclusters, its second derivative (κ-cas in Fig. 4b) revealed a downshifted major minimum somewhat below 1,630 cm^{-1}, and a characteristic weaker band pair above 1,670 cm^{-1} similarly to in the presence of CaP (shown in Fig. 2).

Surface properties of the (α–κ)-casein aggregates (AFM studies)

To reveal whether κ-casein adsorption onto the α-casein surface alters the morphology and elasticity of the aggregates, atomic force microscopic measurements were carried out by recording height images (in tapping mode) on casein multilayers built up step by step (Fig. 5a–e). On the corresponding height profiles plotted in the right column of Fig. 5, it can be seen that the first adsorbed α-casein (α-cas-I) filled up the "bumps" of the polyelectrolyte film surface (compare traces a and b in Fig. 5). Formation of CaP on the α-casein surface somewhat increased the rugosity (Fig. 5c), which was not altered considerably upon the adsorption of the second α-casein layer (α-cas-II) (Fig. 5d). κ-casein—adsorbed in the absence of CaP—decreased somewhat the surface rugosity of the underlying α-cas-II layer (compare Fig. 5e and d). At the same time, however, the κ-casein surface (Fig. 5e) exhibits slightly more pronounced surface nodes as compared with the first α-casein layer—also adsorbed without underlying CaP nanoclusters (α-cas-I in Fig. 5b). These nodes may indicate the appearance of uniformly aggregated structures brought about by κ-casein adsorption onto the "nude" (CaP-free) α-casein surface. (We are aware that this is more an observation than explicit fact, therefore no direct conclusion is based on it.)

One may assume that the protein surfaces, especially the surface of the κ-cas layer shown in Fig. 5, should be rather similar to surfaces of adsorbed native casein micelles. Indeed, Qi obtained similar pictures from native micelles, but more specific comments on the similarities cannot be made because of the lack of height profiles in that publication (Qi 2007).

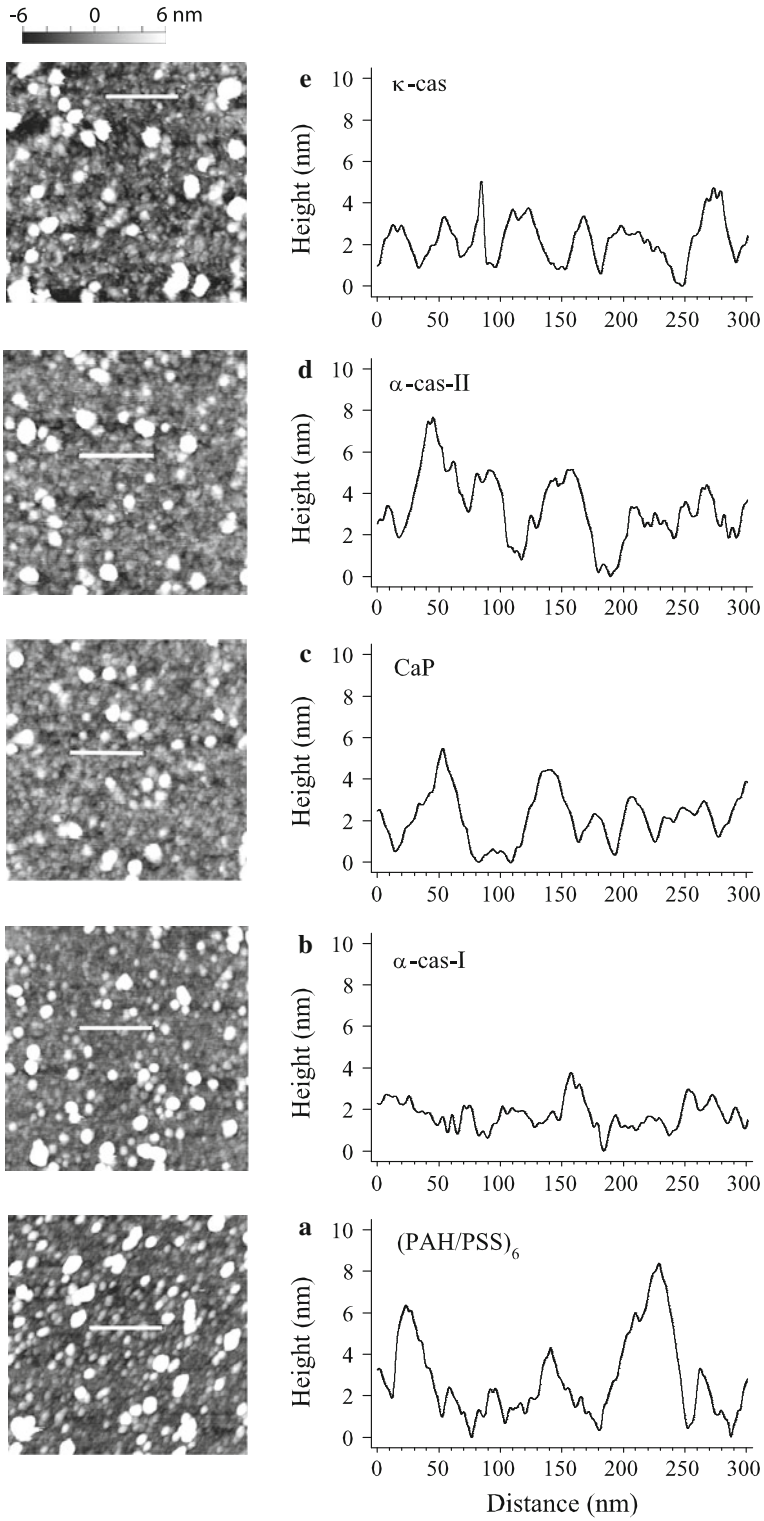

Fig. 5 Height images and height profiles of a step-by-step built casein multilayer. Thorough washing with 10 mM pH 7.0 HEPES buffer separated each step, and the measurements were done in this buffer. *(PAH/PSS)*$_6$, the underlying polyelectrolyte film; *α-cas-I*, the surface of the adsorbed protein multilayer after the first α-casein adsorption; *CaP*, after calcium phosphate nanocluster generation; *α-cas-II*, after the second α-casein adsorption; *κ-cas*, after κ-casein adsorption. On the images, white bars indicate 300-nm traces where the corresponding height profiles, shown on the right, were recorded

The results of measuring the force accompanying the indentation of the cantilever are coherent with the information obtained from the height images and profiles. Figure 6 shows the force measurements on the architecture depicted in Fig. 4a. Upon creating CaP nanoclusters on the first α-casein layer, the protein film becomes more rigid (see CaP curves in Fig. 6), and it softens again, even slightly further, upon the second α-casein adsorption (α-cas-II curves in Fig. 6). Upon adsorbing κ-casein onto the second α-casein layer—without forming CaP nanoclusters in between—some further softening appears. We do not think that this softening can be ascribed specifically to the

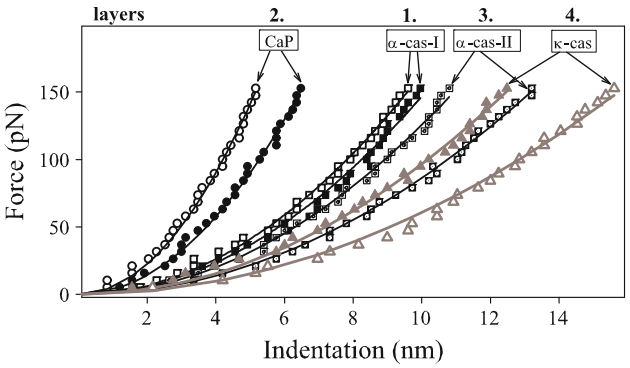

Fig. 6 Force curves recorded upon the indentation of the cantilever of the AFM. At the top of the figure, the numbers indicate the order of the adsorbed layers. To check layer homogeneity, at each layer two datasets were recorded at different locations; each data point is the average of five force measurements. Lines indicate fits according to the Hertz–Sneddon theory (Hertz 1881; Sneddon 1965). Other details are given in our previous publication (Nagy et al. 2010). Note that creating CaP nanoclusters caused significant hardening (higher force at the same indentation means stiffer layer), and that with increasing amount of protein present there is a slight, continuous softening of the film. In this respect, it is worth mentioning that the softening upon κ-casein adsorption is similar to that seen from one α-casein layer to another; i.e. the general physical parameters of the κ- and the α-casein layers should be also similar

properties of κ-casein. Simply, more protein was present in a larger thickness; this might be the most plausible reason, and another proof of κ-casein adsorption onto α-casein surface. [AFM force measurements were carried out on the architecture depicted in Fig. 2a as well (data not shown). There, CaP stiffened uniformly the α- and the κ-casein layers, indicating that their overall physical parameters are similar.]

Discussion

Similarities and differences between the secondary structures of α- and κ-casein

At first glance, the secondary structures of the two caseins look almost identical, as evidenced by the great similarity of the shapes of their amide I′ bands (Fig. 3a). It has to be mentioned, however, that there is a very strong external ordering force in this case, namely the presence of the $(PAH/PSS)_6$ polyelectrolyte film with its negative surface. Therefore, taking into account the intrinsically disordered nature of caseins, we can safely state only that the secondary structures of the α- and the κ-casein seem to be very similar when they are adsorbed onto the negative PSS surface. Indeed, changing the conditions (interaction with CaP, or protein multilayer build-up) reveals that this similarity is limited to the envelope of the amide I′ bands; under the similar envelopes, quite different components with different sensitivity and dynamics may exist. (This situation illustrates very well the problem of protein secondary structure determination from the amide I band by decomposing it into component bands to be assigned to different secondary structural elements.)

The structural differences between α- and κ-casein become more visible when their changes are followed upon the build-up of the protein multilayer (Fig. 2). Here, except for the first protein layer (which is in contact with the polyelectrolyte film on its other side), the protein–protein interactions are decisive. As can be seen, α-casein exhibits very small changes, not only upon α- ↔ α-casein but also upon α- ↔ κ-casein interaction. In contrast, κ-casein is greatly changed upon either α- ↔ κ-casein or κ- ↔ κ-casein interactions (Fig. 2). The appearing dominance of two minima (around 1,670 and 1,630 cm^{-1}) in the second derivative of the amide I′ region of the κ-casein infrared spectrum (Fig. 2b) is indicative of emerging antiparallel β-structures (Arrondo et al. 1993) similar to those always seen upon denaturing-induced protein aggregation (van Stokkum et al. 1995).

Besides analyzing the end-states of the altered α- and κ-casein structures in the protein film, it is also very interesting to see which structural elements are transformed into that denatured-like β-structure. Singular value decomposition (SVD) analysis could reveal that the source native structural elements, which were transformed into β-structure, were different in α- and κ-casein (Fig. 3b). The central frequencies of the lost structural components (i.e., the source of the altering protein segments) are different in α-casein (around 1,656 cm^{-1}) and in κ-casein (around 1,651 cm^{-1}). In contrast to the different source structures, the central frequencies of the emerging β-structure are the same in both caseins (∼1,680 and 1,625 cm^{-1}). This may suggest that the observed β-structure is a more or less uniform end-state for the protein segments involved in it. [It should be noted here that, in the SVD analysis, the assignment of the minima and maxima observed in the s_2 spectra to specific secondary structure elements generally is not possible. Remember that s_2 is not a real infrared spectrum; it is only a vector of a matrix, which, while reflecting the first order of the changes enforced by the external conditions, has to enter a linear combination involving the amplitude vectors (v_i) and the weights (w_i) to provide the infrared spectrum at a given external condition.] Here, however, due to the predominance of the features at frequencies characteristic for β-structures in the protein infrared spectra, this assignment can be rather safely done.

κ-Casein may terminate casein micelle growth

The most remarkable finding of this study is that only κ-casein had the capacity to adsorb onto α-casein without

CaP. In the opposite order, α-casein was not adsorbed onto either α- or κ-casein surface (Fig. 4) without the presence of CaP nanoclusters. Note that κ-casein adsorption is always accompanied by the emergence of a considerable amount of β-structures, while the structure of α-casein remains roughly the same (Figs. 2, 4). It is not clear, however, whether κ-casein suffers this structural change due to interaction with the CaP nanoclusters or with other proteins. The character of the changes appearing in the presence and in the absence of CaP formation was very similar (Figs. 2b, 4b). Even in the absence of CaP nanoclusters on the last α-casein layer, some CaP, due to the incomplete covering of the last α-casein layer (Fig. 4), could remain accessible for the more flexible κ-casein molecules. According to the AFM surface profiles and force measurements, the rugosity (Fig. 5) and dynamic parameters (Fig. 6) of the κ-casein layers were very similar to those of the α-casein layers. Therefore, we think that the fact that κ-casein in these experiments was mostly in the form of disulfide bridge-connected polymers (two cysteins/molecule) did not affect the experiments or the conclusions drawn from them.

These results suggest that a similar phenomenon might apply in vivo; κ-caseins adsorbing onto α-casein may provide such a casein micelle surface, which cannot bind any more casein, thus the growth of the casein micelle terminates. In addition, a surface made from κ-casein could provide the hairy structure needed for the solubility and stability of casein micelles in vivo.

Acknowledgments Hungarian Research Foundation (OTKA) grants K-75818 (to B.Sz.) and K-81180 (to K.N. and G.V.) supported this work. The authors thank S. Bankó and Z. Kucsma for checking the purity of the proteins.

References

Arrondo JL, Muga A, Castresana J, Goni FM (1993) Quantitative studies of the structure of proteins in solution by Fourier-transform infrared spectroscopy. Prog Biophys Mol Biol 59:23–56

Butt HJ, Jaschke M (1995) Calculation of thermal noise in atomic force microscopy. Nanotechnology 6:1–7

De Kruif CG, Zhulina EB (1996) [kappa]-casein as a polyelectrolyte brush on the surface of casein micelles. Colloids Surf A Physicochem Eng Asp 117:151–159

Decher G (1997) Fuzzy nanoassemblies: toward layered polymeric multi composites. Science 277:1232–1237. doi:10.1126/science.277.5330.1232

Farrell HM, Cooke PH, Wickham ED, Piotrowski EG, Hoagland PD (2003) Environmental influences on bovine kappa-casein: reduction and conversion to fibrillar (amyloid) structures. J Prot Chem 22:259–273

Farrell JHM, Malin EL, Brown EM, Qi PX (2006) Casein micelle structure: what can be learned from milk synthesis and structural biology? Curr Opin Colloid Interface Sci 11:135–147

Farrell HM, Brown EM, Malin EL (2012) Higher order structures of the caseins: a paradox? In: McSweeney PLH, Fox PF (eds) Advanced dairy chemistry. Springer, New York

Florin EL, Rief M, Lehmann H, Ludwig M, Dornmair C, Moy VT, Gaub HE (1995) Sensing specific molecular interactions with the atomic force microscope. Biosens Bioelectron 10:895–901

Henry ER, and Hofrichter J (1992) Singular value decomposition: application to analysis of experimental data. Method Enzymol 210:129–192

Hertz MG (1881) Über die Berührung Fester Elastischer Körper. J Reine Angew Math 92:156–171

Holt C, Horne DS (1996) The hairy casein micelle: evolution of the concept and its implications for dairy technology. Neth Milk Diary J 50:85–111

Holt C, De Kruif CG, Tuinier R, Timmins PA (2003) Substructure of bovine casein micelles by small-angle X-ray and neutron scattering. Curr Opin Colloid Interface Sci 213:275–284

Horne DS (2002) Casein structure, self-assembly and gelation. Curr Opin Colloid Interface Sci 7:456–461

Horne DS (2006) Casein micelle structure: models and muddles. Curr Opin Colloid Interface Sci 11:148–153

Hutter JL, Bechhoefer J (1993) Calibration of atomic-force microscope tips. Rev Sci Instrum 64:1868–1873

Kota Z, Debreczeny M, Szalontai B (1999) Separable contributions of ordered and disordered lipid fatty acyl chain segments to nu CH_2 bands in model and biological membranes: a Fourier transform infrared spectroscopic study. Biospectroscopy 5:169–178

Mallat S (1998) In: a wavelet tour of signal processing. Academic, San Diego

Müller-Buschbaum P, Gebhardt R, Roth SV, Metwalli ZE, Doster W (2007) Effect of calcium concentration on the structure of casein micelles in thin films. Biophys J 93:960–968

Nagy K, Pilbat AM, Groma G, Szalontai B, Cuisinier FJG (2010) Casein aggregates built step-by-step on charged polyelectrolyte film surfaces are calcium phosphate-cemented. J Biol Chem 285:38811–38817

Palmer DS, Christensen AU, Sørensen J, Celik L, Qvist KB, Schiøtt B (2010) Bovine chymosin: a computational study of recognition and binding of bovine kappa-casein. Biochemistry 49:2563–2573. doi:10.1021/bi902193u

Qi PX (2007) Studies of casein micelle structure: the past and the present. Lait 87:363–383. doi:10.1051/lait:2007026

Schwinte P, Voegel JC, Picart C, Haikel Y, Schaaf P, Szalontai B (2001) Stabilizing effects of various polyelectrolyte multilayer films on the structure of adsorbed/embedded fibrinogen molecules: an ATR-FTIR study. J Phys Chem B 105:11906–11916

Sneddon IN (1965) The relation between load and penetration in the axisymmetric boussinesq problem for a punch of arbitrary profile. Int J Eng Sci 3:47–57

Szalontai B (2009) Membrane protein dynamics: limited lipid control. PMC Biophys 2:1. doi:10.1186/1757-5036-2-1

Tompa P, Fuxreiter M (2008) Residual structure and binding functions of intrinsically disordered proteins. In: Unfolded proteins. From denatured to intrinsically disordered. NOVA Science Publishers Inc: New York, pp 213–236

van Stokkum IH, Linsdell H, Hadden JM, Haris PI, Chapman D, Bloemendal M (1995) Temperature-induced changes in protein structures studied by Fourier transform infrared spectroscopy and global analysis. Biochemistry 34:10508–10518

Walstra P (1990) On the stability of casein micelles. J Dairy Sci 73:1965–1979

Walstra P (1999) Casein sub-micelles: do they exist? Int Dairy J 9:189–192

Walstra P, Jennes R (1984) Dairy chemistry and physics. Wiley, New York

Waugh DF (1970) Formation and structure of casein micelles. Academic, London